Journal of Molecular Spectroscopy 266 (2011) 86–91

Contents lists available at ScienceDirect

Journal of Molecular Spectroscopy

journal homepage: www.elsevier.com/locate/jms

Fourier transform emission spectroscopy of the $E^2\Pi$–$X^2\Sigma^+$ transition of CaH and CaD

R.S. Ram [a,b], K. Tereszchuk [a], I.E. Gordon [c], K.A. Walker [d], P.F. Bernath [a,b,*]

[a] Department of Chemistry, University of York, Heslington, York YO10 5DD, UK
[b] Department of Chemistry, University of Arizona, Tucson, AZ 85721, USA
[c] Harvard-Smithsonian Center for Astrophysics, Cambridge, MA 02138, USA
[d] Department of Physics, University of Toronto, Toronto, Canada, ON M5S 1A7

ARTICLE INFO

Article history:
Received 26 January 2011
In revised form 8 March 2011
Available online 15 March 2011

Keywords:
Stellar atmospheres
Electronic spectra
Rotational analysis
Equilibrium constants

ABSTRACT

The emission spectra of CaH and CaD have been recorded at high resolution using a Fourier transform spectrometer and bands belonging to the $E^2\Pi$–$X^2\Sigma^+$ transition have been measured in the 20 100–20 700 cm^{-1} region. A rotational analysis of 0–0 and 1–1 bands of both the isotopologues has been carried out. The present measurements have been combined with the previously available pure rotation and vibration–rotation data to provide improved spectroscopic constants for the $E^2\Pi$ state. The constants $\Delta G(1/2) = 1199.8867(34)$ cm^{-1}, $B_e = 4.345032(49)$ cm^{-1}, $\alpha_e = 0.122115(92)$ cm^{-1}, $r_e = 1.986633(11)$ Å for CaH, and $\Delta G(1/2) = 868.7438(46)$ cm^{-1}, $B_e = 2.212496(51)$ cm^{-1}, $\alpha_e = 0.036509(97)$ cm^{-1}, $r_e = 1.993396(23)$ Å for CaD have been determined.

1. Introduction

Calcium hydride is an important astrophysical molecule and has long been identified in sunspots through several band heads in the orange and red [1,2]. The same bands are seen in M dwarfs, but weakly in the spectra of M giants [3]. The formation of CaH in stellar atmospheres is strongly influenced by gas pressure, thus CaH bands can be used as a luminosity indicator for cool stars [4–6]. CaH can also be used to determine the surface gravity of cool stars [4–6].

Absorption in CaH bands is also an important opacity source in brown dwarfs and can be used to study these substellar objects [7,8]. Brown dwarfs are smaller than stars and are not massive enough to burn hydrogen in their cores, although nuclear fusion of other nuclei such as deuterium and lithium is still possible. The CaH bands are particularly strong in M dwarfs and used to identify M subdwarfs [9] and L subdwarfs [10,11]. Subdwarfs have very low abundances of heavy elements compared to normal stars like the Sun. In M-type subdwarfs metal hydrides such as CaH are enhanced relative to metal oxides such as TiO because they contain a single heavy element as compared to two heavy elements for the oxides [12].

In part because of the astrophysical importance of CaH, a series of laboratory spectroscopic studies of the molecule have been carried out over the past several decades including: the diode laser measurements of the 1–0 to 4–3 vibration–rotation bands of CaH and CaD [13], the measurements of the fundamental and first hot band of CaH using a Fourier transform spectrometer [14] and measurement of the pure rotational transitions in the ground electronic state [15,16]. A summary of previous spectroscopic studies of CaH has been provided in the recent work by Shayesteh et al. [17], who reported on an extensive set of vibration–rotation measurements of CaH using a Fourier transform spectrometer. In this work many additional transitions were measured compared to those reported earlier [13,14] for the 1–0 to 4–3 vibration–rotation bands of CaH.

Steimle and co-workers have carried out a number of recent high precision measurements on the electronic transitions of CaH and CaD [18–21], motivated in part by the successful magnetic trapping of CaH [22]. In one publication they reported the study of the $A^2\Pi/B^2\Sigma^+$–$X^2\Sigma^+$ systems using a supersonic molecular beam and laser-induced fluorescence, and modeled the interaction between the $A^2\Pi(v = 1)$ and $B^2\Sigma^+(v = 0)$ vibronic levels [18]. They also studied the Stark effect in the 0–0 band of the $A^2\Pi$–$X^2\Sigma^+$ transition of CaH [19] and in the 0–0 band of the $B^2\Sigma^+$–$X^2\Sigma^+$ transition of CaD [21] in order to determine the permanent dipole moments of the $B^2\Sigma^+$, $A^2\Pi$ and $X^2\Sigma^+$ states. In another study they investigated the Zeeman effect in the ground and low-lying $A^2\Pi$ and $B^2\Sigma^+$ electronic states of CaH [20].

There are a number of theoretical studies available for CaH [23–29]. The studies by Honjou et al. [23], Chambaud and Levy [24], Boutalib et al. [25] and Leininger and Jeung [26] were focussed on the calculation of spectroscopic properties and potential energy curves of the low-lying electronic states. Weck et al. [27] have calculated theoretical line lists for the electronic transitions from the low-lying excited electronic states to the ground state of CaH for astronomical purposes. Their study was aimed at providing synthetic spectra which can be compared with the spectra of cool

* Corresponding author at: Department of Chemistry, University of York, Heslington, York YO10 5DD, UK. Fax: +44 (0) 1904 432516.
E-mail address: pfb500@york.ac.uk (P.F. Bernath).

0022-2852/$ - see front matter © 2011 Elsevier Inc. All rights reserved.
doi:10.1016/j.jms.2011.03.009

stars and brown dwarfs to deduce physical parameters such as the effective temperature and surface chemical composition. The recent theoretical studies by Holka and Urban [28] and Kerkines and Mavridis [29] have predicted the molecular properties and dipole moments for the ground and some low-lying electronic states of CaH.

Most of the higher-lying electronic states of CaH, however, are not well characterized and high resolution data for some states are still lacking. The $E^2\Pi$ state of CaH is known through the observation of the $E^2\Pi$–$X^2\Sigma^+$ transition in 1932 by Grundström [30] and a subsequent study by Watson and Weber [31] who carried out a rotational analysis of the 0–0 band using a spectrum recorded at a moderate resolution. The observation of the corresponding transition for CaD is still lacking. In this paper we report the rotational analysis of the $E^2\Pi$–$X^2\Sigma^+$ transition of CaH and CaD using spectra recorded using a Fourier transform spectrometer. The bands belonging to this transition were observed while recording the high resolution spectra of the $A^2\Pi$–$X^2\Sigma^+$ and $B^2\Sigma^+$–$X^2\Sigma^+$ transitions.

2. Experimental

The emission spectra of CaH were produced in a source which is a combination of a high temperature furnace and an electrical discharge source [17]. The furnace is made of high temperature alumina tube which is fitted with two cylindrical stainless steel electrodes at the both ends of the tube which is cooled by continuous flow of water through the outer jacket over the electrodes. The furnace is used to produce sufficient metal vapor which is reacted with a trace of hydrogen to produce the metal hydride molecules. In the present case about 50 g of calcium metal was placed inside the central part of the alumina tube and was heated to a temperature of approximately 780 °C. The calcium metal vapor was then reacted with about 1 Torr of hydrogen to produce CaH molecules in the discharge. A few Torr of Ar gas were used as a carrier gas. For CaD, D_2 gas was used instead of hydrogen. The emission from the furnace was focused onto the entrance aperture of a Bruker IFS 120 HR Fourier transform spectrometer. A visible quartz beam splitter and a photomultiplier detector were used, and the spectra were recorded in the 16 800–31 600 cm^{-1} region at a resolution of 0.04 cm^{-1}. About 90 scans were co-added in about two hours of integration to observe these bands with sufficient signal-to-noise ratio.

The observed bands were readily identified as due to CaH using the published band head positions. The spectral line positions were measured using a data reduction program called WSPECTRA written by M. Carleer of the Université Libre de Bruxelles. The peak positions were determined by fitting a Voigt line shape function to each experimental feature. Our spectra also contained Ar atomic lines which were used for calibration using the Ar line measurements by Whaling et al. [32]. The molecular lines appear with approximate widths of ~0.09 cm^{-1} and a maximum signal-to-noise ratio of about 46:1 for the strongest Q lines of the 0–0 bands of CaH and CaD. The precision of measurements of the molecular lines is expected to be better than ±0.003 cm^{-1}. However, the precision of measurements of the weaker lines in the 1–1 bands, which are frequently overlapped with the much stronger 0–0 bands particularly in the Q branch regions, is expected to be some what lower.

3. Results and discussion

The spectrum of the $E^2\Pi$–$X^2\Sigma^+$ transition is located in the 20 100–20 700 cm^{-1} region. The spectra of both isotopologues consist of strongly diagonal bands with very weak $\Delta v \neq 0$ bands. We found the 0–0 band strongest in intensity followed by the 1–1 band which is ~20% of the intensity of the 0–0 band. The rotational structure of the 2–2 band could not be measured because of its much weaker intensity. This transition involves a $^2\Pi$ upper state with a small spin–orbit splitting so the excited state tends towards Hund's case (b) coupling. A Hund's case (a) $^2\Pi$–$^2\Sigma^+$ transition results in six main branches and six satellite branches; however, our spectrum for each band consists of only 2P, 2Q and 2R branches with the Q branches being the most intense. Satellite branches were not observed even in the strongest 0–0 bands. The observed branches in the 0–0 and 1–1 bands have been assigned as P_1, Q_1, R_1, P_2, Q_2, R_2 and labeled as P_{1ee}, Q_{1fe}, R_{1ee}, P_{2ff}, Q_{2ef}, and R_{2ff}, respectively, following the usual energy level diagram of a $A^2\Pi$–$X^2\Sigma^+$ transition. Our assignment was made by comparing the lower state combination differences to the precisely known values for the *e*- and *f*-parity levels of the $X^2\Sigma^+$ state from the pure rotation and vibration–rotation studies [13–17]. Our analysis suggests that the labels of branches by Watson and Weber [31] must be changed from P_1, Q_1, R_1, P_2, Q_2, R_2 to P_2, Q_2, R_2, P_1, Q_1, R_1, respectively. The lines in the R and P branches have a nearly constant spacing resulting in an open structure without a band head in either branch. This is because of the near equality of rotational constants in the lower and upper electronic states.

A compressed portion of the spectrum of CaH is presented in Fig. 1 in which the strong Q heads of the 0–0 and 1–1 bands have been marked. As can be seen, the 1–1 band is much weaker than the 0–0 band. Also, we note that the P branch lines are weaker in intensity than the R branch lines (see Fig. 1). We have measured the rotational lines up to $P_{1ee}(26.5)$, $Q_{1fe}(25.5)$, $R_{1ee}(28.5)$, $P_{2ff}(25.5)$, $Q_{2ef}(23.5)$ and $R_{2ff}(28.5)$ in the 0–0 band of CaH. In the 1–1 band, we have assigned the rotational lines up to $P_{1ee}(18.5)$, $Q_{1fe}(14.5)$, $R_{1ee}(16.5)$, $P_{2ff}(16.5)$, $Q_{2ef}(14.5)$ and $R_{2ff}(15.5)$. An expanded portion of the spectrum of the R branch region is presented in Fig. 2 where some R lines of the 0–0 and 1–1 bands have been marked. The rotational lines of CaH are free from perturbations except a local perturbation at $F_{1e}(13.5)$ of the excited state which shifts the corresponding R and P lines by −0.07 cm^{-1}. The 1–1 band, however, is affected by interactions at lower J as well as some higher J values of the upper state. The lines affected by perturbations were given lower weights in the final fit.

The spectrum of CaD is very similar to that of CaH. In this case we have identified rotational lines up to $P_{1ee}(33.5)$, $Q_{1fe}(25.5)$, $R_{1ee}(37.5)$, $P_{2ff}(33.5)$, $Q_{2fe}(32.5)$ and $R_{2ff}(35.5)$ in the 0–0 band. A portion of the Q branch of the 0–0 band of CaD is presented in Fig. 3, marking some rotational lines of the Q_1 and Q_2 branches. The effects of interactions can also be seen from the observed minus calculated differences for the 0–0 and 1–1 bands of CaD. The effect of interactions is particularly apparent in the 1–1 band where Q_1 branch appears as usual but the Q_2 lines are compressed and packed into a ~2 cm^{-1} range. These Q_2 lines were not included in the least-squares fit.

The spectroscopic constants for the ground and excited vibrational levels were determined by fitting the observed rotational lines of different bands with the effective N^2 Hamiltonian of Brown et al. [33]. The matrix elements of this Hamiltonian for $^2\Sigma^+$ and $^2\Pi$ states are provided, for example, by Douay et al. [34] and Amiot et al. [35]. In the final fit the vibration–rotation [13,14,17] and pure rotational [15,16] measurements of CaH and CaD from the previous studies were also combined with our present measurements. Our analysis provides a good fit for the 0–0 band of CaH while some rotational lines of the 1–1 were affected by interactions in the excited state and were given lower weights. For CaD also some of the rotational lines of the 0–0 and 1–1 bands affected by interactions in the excited state were given lower weights. The measurements of the 0–0 band of CaH along with obs.-calc. residuals are provided in Table 1. The output of the final fits of the CaH and CaD bands

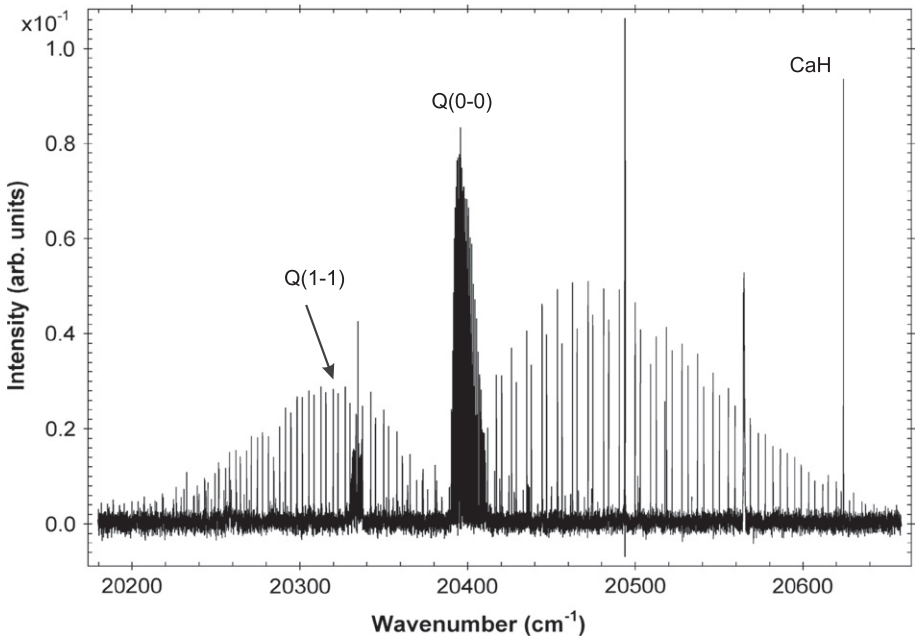

Fig. 1. A compressed portion of the spectrum of the $E^2\Pi$–$X^2\Sigma^+$ electronic transition of CaH with the Q heads of the 0–0 and 1–1 bands marked.

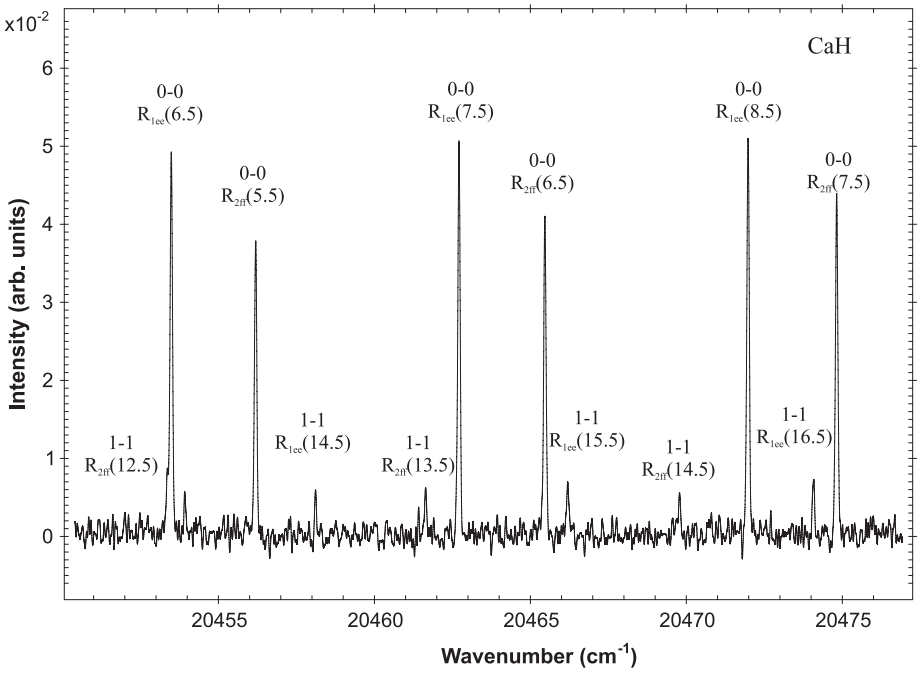

Fig. 2. An expanded portion of the spectrum of CaH with some R lines of the 0–0 and 1–1 bands marked.

listing fitted constants, the observed transition wavenumbers and their obs.-calc. residuals are provided in Supplement 1 and the calculated term values for the observed vibrational levels of the two states of CaH and CaD are provided in Supplement 2. The supplement files are available on ScienceDirect (www.sciencedirect.com) and as part of the Ohio State University Molecular Spectroscopy Archives (http://msa.lib.ohio-state.edu/jmsa_hp.htm). The spectroscopic constants for the ground and excited electronic states of CaH and CaD are provided in Table 2. As can be seen, in addition to the large magnitudes of γ_v, q_v and p_v, many higher order constants such as γ_{Dv}, γ_{Hv}, H_v, q_{Dv} and p_{Dv} were required to minimize the standard deviation of the fit. This observation is an indicative of the interactions in the excited state. The $D^2\Sigma^+$ state which is observed only about 2132 cm^{-1} above the $E^2\Pi$ state is a potential candidate for this interaction.

We have used the spectroscopic constants provided in Table 2 to determine the equilibrium constants of the excited electronic states of CaH and CaD using the standard equations. The equilibrium constants are provided in Table 3. The equilibrium rotational constants of B_e = 4.345032(49) cm^{-1} and 2.212496(51) cm^{-1} for the $E^2\Pi$ state of CaH and CaD provide the equilibrium bond lengths of 1.986633(11) Å and 1.993396(23) Å, respectively, for the $E^2\Pi$

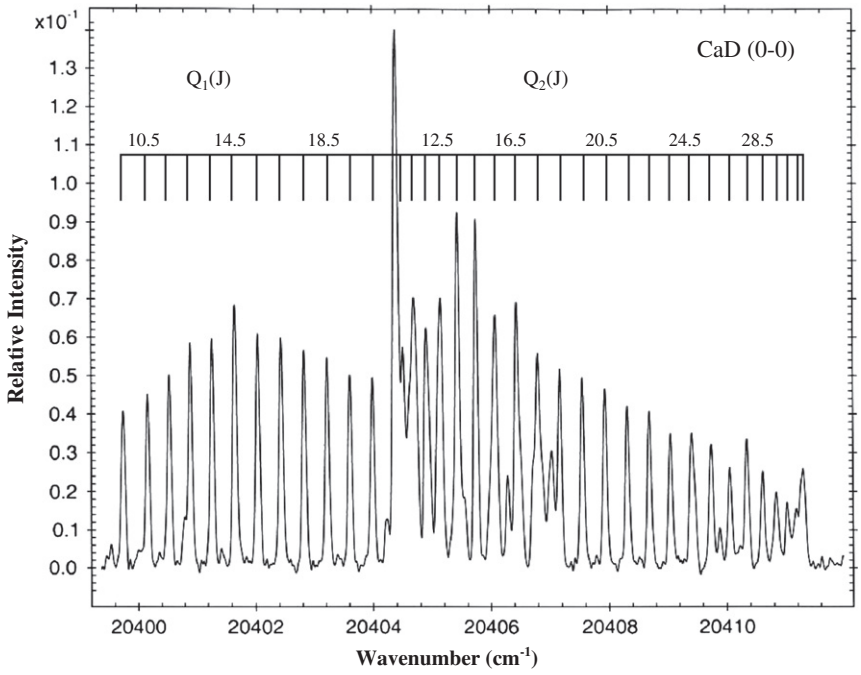

Fig. 3. An expanded portion of the 0–0 band of CaD with some rotational lines in the Q branches marked.

Table 1
Observed rotational line positions (in cm^{-1}) in the 0–0 band of the $E^2\Pi$–$X^2\Sigma^+$ transition of CaH.

J	R_{1ee}	O–C	Q_{1fe}	O–C	P_{1ee}	O–C	R_{2ff}	O–C	Q_{2ef}	O–C	P_{2ff}	O–C
0.5	20398.8786	0.0289	20389.1630	0.0037			20411.9354	−0.0006				
1.5	20408.0347	−0.0022	20390.4243	0.0061	20380.6429	0.0126	20420.2706	0.0060				
2.5	20417.0814	0.0014	20391.1082	0.0033	20373.4444	0.0037	20428.9641	0.0012	20394.7762	−0.0052	20369.7156	−0.0029
3.5	20426.1091	−0.0004	20391.6216	0.0016	20365.7324	0.0000	20437.8820	−0.0007	20394.9221	0.0070	20361.1756	0.0020
4.5	20435.1725	−0.0007	20392.1014	0.0004	20357.9049	0.0026	20446.9560	−0.0009	20395.2543	−0.0005	20353.0272	−0.0023
5.5	20444.2857	−0.0026	20392.6014	−0.0001	20350.0900	0.0004	20456.1630	0.0144	20395.7364	−0.0030	20345.1534	0.0069
6.5	20453.4584	−0.0005	20393.1427	−0.0014	20342.3509	0.0001	20465.4333	0.0011	20396.3380	0.0010	20337.4665	−0.0003
7.5	20462.6817	−0.0002	20393.7357	−0.0018	20334.7126	0.0003	20474.7876	0.0001	20397.0330	0.0058	20329.9806	0.0191
8.5	20471.9498	−0.0005	20394.3825	−0.0014	20327.1800	−0.0064	20484.1950	−0.0015	20397.7918	−0.0034	20322.6171	0.0029
9.5	20481.2520	−0.0029	20395.0761	−0.0052	20319.7794	0.0005	20493.6421	−0.0003	20398.6240	−0.0038	20315.4129	−0.0001
10.5	20490.5829	−0.0013	20395.8219	−0.0036	20312.4933	0.0018	20503.1065	−0.0021	20399.5088	−0.0047	20308.3526	0.0040
11.5	20499.9226	−0.0032	20396.6070	−0.0031	20305.3205	−0.0026	20512.5717	−0.0069	20400.4374	−0.0035	20301.4102	−0.0022
12.5	20509.1921	−0.0738	20397.4217	−0.0061	20298.2684	−0.0027	20522.0409	0.0055	20401.3928	−0.0057	20294.5964	0.0002
13.5	20518.5952	0.0055	20398.2555	−0.0144	20291.3285	−0.0025	20531.4713	0.0094	20402.3789	0.0040	20287.8853	−0.0064
14.5	20527.8827	0.0010	20399.1329	0.0059	20284.4218	−0.0756	20540.8399	−0.0006	20403.3704	0.0123	20281.2982	0.0081
15.5	20537.1284	0.0025	20399.9898	0.0009	20277.7665	0.0028	20550.1522	−0.0009	20404.3496	0.0137	20274.7817	−0.0005
16.5	20546.3055	0.0007	20400.8524	0.0079	20271.1246	0.0024	20559.3809	−0.0003	20405.2932	−0.0022	20268.3582	0.0000
17.5	20555.4042	0.0030	20401.6832	0.0012	20264.5677	0.0029	20568.5058	0.0003	20406.2283	0.0047	20262.0035	−0.0043
18.5	20564.3976	0.0012	20402.4894	0.0003	20258.0859	0.0040	20577.5051	−0.0013	20407.1201	0.0138	20255.7189	−0.0012
19.5	20573.2707	−0.0006	20403.2542	0.0016	20251.6828	0.0194	20586.3646	0.0016	20407.9261	−0.0033	20249.4930	0.0099
20.5	20582.0008	−0.0049	20403.9538	−0.0050	20245.2999	0.0014	20595.0465	−0.0078	20408.6652	−0.0125	20243.2844	−0.0002
21.5	20590.5779	−0.0011	20404.5916	−0.0012	20238.9773	0.0021	20603.5567	−0.0011	20409.3330	−0.0022	20237.1119	0.0010
22.5	20598.9636	−0.0055	20405.1385	−0.0007	20232.6668	−0.0139	20611.8450	−0.0052	20409.8831	−0.0019	20230.9430	−0.0049
23.5	20607.1408	−0.0123	20405.5768	−0.0047	20226.3870	−0.0140	20619.9167	0.0100	20410.3128	0.0037	20224.7726	−0.0073
24.5	20615.1077	0.0013	20405.9064	0.0045	20220.1159	−0.0051	20627.7145	0.0132			20218.5878	−0.0025
25.5	20622.8079	0.0046	20406.0783	−0.0032	20213.8093	−0.0152	20635.2163	0.0106			20212.3702	0.0094
26.5	20630.2268	0.0109			20207.5095	0.0161	20642.3757	−0.0143				
27.5	20637.3279	0.0136					20649.2189	−0.0027				
28.5	20644.0566	−0.0096					20655.6617	−0.0032				

Note: O–C are observed minus calculated wavenumbers in the units of cm^{-1}.

state. Relatively large difference in the equilibrium bond lengths of the $E^2\Pi$ states of CaH and CaD is likely due to interaction of the $v = 0$ and 1 vibrational levels with the close-lying levels of the $B^2\Sigma^+$ or $D^2\Sigma^+$ electronic states. We were not able to determine the equilibrium vibrational constants because of the lack of experimental spectroscopic constants for the $v \geqslant 2$ vibrational levels. However the $\Delta G(½)$ value of 1199.8867(34) cm^{-1} was obtained for the $E^2\Pi$ state of CaH. Watson and Weber [31] have determined vibrational constants $\omega_e = 1248.6\ cm^{-1}$ and $\omega_e x_e = 21.8\ cm^{-1}$ using the Q head positions of the 0–0, 1–1 and 2–2 bands and the known ground state vibrational intervals. These values provide $\Delta G(½) = 1205.2\ cm^{-1}$ compared to our experimental value of 1199.8867(34) cm^{-1}. The theoretical values of the equilibrium vibrational constant of the $E^2\Pi$ state of CaH are, 1085 cm^{-1} [23],

Table 2
Spectroscopic constants (in cm^{-1}) of the $X^2\Sigma^+$ and $E^2\Pi$ electronic states of CaH and CaD.

Constants	CaH			
	$X^2\Sigma^+$		$E^2\Pi$	
	$v = 0$	$v = 1$	$v = 0$	$v = 1$
T_v	0.0	1260.12780(20)	20392.38995(80)	21592.2766(33)
A_v	–	–	23.9515(32)	25.198(12)
B_v	4.22868970(66)	4.1317211(35)	4.283974(17)	4.161859(90)
$D_v \times 10^4$	1.850744(76)	1.84867(17)	2.25667(88)	2.2523(69)
$H_v \times 10^8$	0.6697(11)	0.6663(26)	1.503(17)	−1.59(16)
$L_v \times 10^{12}$	−0.3411(42)	−0.349(12)	−4.31(10)	–
γ_v	0.0435653(18)	0.042091(22)	−0.15289(17)	−0.18386(73)
$\gamma_{Dv} \times 10^4$	−0.05119(84)	−0.05076(89)	0.4561(76)	2.008(41)
$\gamma_{Hv} \times 10^8$	–	–	−0.512(84)	–
$q_v \times 10^2$	–	–	1.62357(70)	1.2610(56)
$q_{Dv} \times 10^6$	–	–	−3.667(15)	2.26(40)
$p_v \times 10^2$	–	–	1.817(18)	−7.553(89)
$p_{Dv} \times 10^4$	–	–	−0.0816(45)	2.771(68)
	CaD			
T_v	0.0	910.30028(27)	20400.6198(21)	21269.3636(41)
A_v	–	–	23.124(15)	24.575(14)
B_v	2.17694673(56)	2.1413675(32)	2.194241(16)	2.155932(96)
$D_v \times 10^5$	4.8849(11)	4.8776(11)	5.6325(33)	6.343(21)
$H_v \times 10^9$	0.9207(79)	0.8942(70)	1.570(19)	3.182(92)
γ_v	0.0224099(50)	0.021799(21)	−0.08726(56)	−0.1365(15)
$\gamma_{Dv} \times 10^5$	–	–	3.62(13)	4.40(35)
$\gamma_{Hv} \times 10^8$	–	–	−1.546(80)	−2.73(35)
$q_v \times 10^3$	–	–	5.4885(92)	−0.34(20)
$q_{Dv} \times 10^6$	–	–	−1.981(20)	4.69(42)
$p_v \times 10^2$	–	–	3.210(29)	−7.97(21)
$p_{Dv} \times 10^6$	–	–	−9.15(76)	–

Note: Numbers in parentheses are one standard deviation in the last digits quoted.

Table 3
Equilibrium spectroscopic constants (in cm^{-1}) of the $E^2\Pi$ electronic states of CaH and CaD.

Constants	CaH	CaD
$\Delta G(½)$	1199.8867(34)	868.7438(46)
B_e	4.345032(49)	2.212496(51)
α_e	0.122115(92)	0.036509(97)
r_e (Å)	1.986633(11)	1.993396(23)

Note: Numbers in parentheses are one standard deviation in the last digits quoted.

1218 cm^{-1} [24] 1245 cm^{-1} [25] and 1232 cm^{-1} [26] from the recent calculations. The rotational constants obtained in this work agree reasonably well with those reported by Watson and Weber [31] except for the spin–orbit splitting constant for the $E^2\Pi$ state. Our analysis provides $A_0 = 23.9515(32)$ cm^{-1} and $A_1 = 25.198(12)$ cm^{-1} while $A_0 = 9.3$ cm^{-1} was reported by Watson and Weber [31]. This value was, in fact, obtained from a rough estimate, rather than a fit. The corresponding values of $A_0 = 23.124(15)$ cm^{-1} and $A_1 = 24.575(14)$ cm^{-1} have been determined for CaD in the present work.

A number of electronic states ($X^2\Sigma^+$, $A^2\Pi$, $B^2\Sigma^+$, $E^2\Pi$, $D^2\Sigma^+$) of CaH have been known for a long time and the electronic configurations provide a simple picture of the electronic structure. But in actual practice the interpretation of the observed spectra and the electronic structure is much more difficult because of interactions between the $A^2\Pi$ and $B^2\Sigma^+$ states, existence of a double well in the $B^2\Sigma^+$ state because of an avoided crossing, and interaction between the $E^2\Pi$ and $D^2\Sigma^+$ states. The earlier theoretical studies have, therefore, focussed on the potential curves for these states in addition to predicting their spectroscopic properties. The *ab initio* calculations of Honjou et al. [23] have provided the following dominant electron configurations for the low-lying electronic states of CaH:

$$6\sigma^2 7\sigma \quad X^2\Sigma^+ \tag{1}$$
$$6\sigma^2 3\pi \quad A^2\Pi \tag{2}$$
$$6\sigma^2 8\sigma \quad B^2\Sigma^+ \tag{3}$$
$$6\sigma^2 4\pi \quad E^2\Pi \tag{4}$$
$$6\sigma 7\sigma^2 \quad D^2\Sigma^+ \tag{5}$$

The $X^2\Sigma^+$ state dissociates to the [Ca ($4s^2$, ^1S) + H(^2S)] limit, the $A^2\Pi$ and $B^2\Sigma^+$ states correlate to [Ca(4s4p, ^3P) + H(^2S)] and the $E^2\Pi$ and $D^2\Sigma^+$ states correlate to the next excited [Ca(4s3d, ^3D) + H(^2S)] atomic limits. In addition, a $^2\Delta$ state with similar spectroscopic constants as the other low-lying states has been predicted near 21 670 cm^{-1} [23]. This state correlates to [Ca(4s3d, ^3D) + H(^2S)] and has not been observed experimentally so far. Chambaud and Levy [24] and Leininger and Jeung [26] have performed calculations for a number of higher-lying electronic states correlating to more highly excited atomic states. As the theoretical results and experimental observations suggest, the $D^2\Sigma^+$ state is only 2132 cm^{-1} higher than the $E^2\Pi$ state. The observed perturbations in the $v = 0$ and 1 vibrational levels of the $E^2\Pi$ state are likely caused by the interaction with the $D^2\Sigma^+$ state or the lower-lying $B^2\Sigma^+$ state.

In a study of CaH, Bell et al. [36] obtained a rotational analysis of the $D^2\Sigma^+$-$X^2\Sigma^+$ transition and revised its vibrational assignment. This analysis reduced the vibrational frequency of the $D^2\Sigma^+$ state by a factor of two. The anomalies in the rotational structure of the $D^2\Sigma^+$ state were explained by strong homogeneous interaction with the higher vibrational levels of the $B^2\Sigma^+$ state. A comparison of our $E^2\Pi$ state term values for CaH to those of the $D^2\Sigma^+$ vibrational levels [36] indicates that the $D^2\Sigma^+$ state is not responsible for perturbations in the $v = 1$ vibrational level of the $E^2\Pi$ state. As suggested previously, the perturbations observed in the $v = 1$ level of the $E^2\Pi$ state are most probably caused by the higher vibrational levels of the $B^2\Sigma^+$ state.

The previous analysis of the $D^2\Sigma^+$–$X^2\Sigma^+$ transition of CaD [37] has attributed a number of local perturbations to the interaction of the $D^2\Sigma^+$ state with the $E^2\Pi$ state. We find that the $E^2\Pi$ $v = 0$ vibrational level interacts with $D^2\Sigma^+$ $v = 0$ at around $N = 38$ where rotational lines of both the transitions become very weak. Just as in the case of CaH the observed perturbations in the $v = 1$ vibrational level of the $E^2\Pi$ state of CaD are most likely due its interaction with the low-lying $B^2\Sigma^+$ state.

4. Conclusion

The emission spectra of CaH and CaD have been investigated in the visible region using a Fourier transform spectrometer. The rotational structure of the 0–0 and 1–1 bands of the $E^2\Pi$–$X^2\Sigma^+$ transition of the two isotopologues has been analysed and improved spectroscopic constants for the excited state have been derived by combining the available infrared pure rotation [15,16] and vibration–rotation [13,14,17] measurements with the present measurements. The observed perturbations in the excited state are probably due to interactions with the close-lying $D^2\Sigma^+$ state and the lower-lying $B^2\Sigma^+$ state.

Acknowledgments

We thank the Leverhulme Trust for financial support through a Research Project Grant. The spectra of CaH and CaD were recorded when Tereszchuk, Gordon, Walker and Bernath were at the University of Waterloo.

Appendix A. Supplementary material

Supplementary data associated with this article can be found, in the online version, at doi:10.1016/j.jms.2011.03.009.

References

[1] C.M. Olmsted, Astrophys. J. 27 (1908) 66–69.
[2] A. Eagle, Astrophys. J. 30 (1909) 231–236.
[3] Y. Öhman, Astrophys. J. 80 (1934) 171–180.
[4] J.R. Mould, Astrophys. J. 207 (1976) 535–544.
[5] J.R. Mould, R.E. Wallis, Mon. Not. Roy. Astron. Soc. 181 (1977) 625–635.
[6] B. Barbuy, R.P. Schiavon, J. Gregorio-Hetem, D.P. Singh, C. Batalha, Astron. Astrophys. Suppl. 101 (1993) 409–413.
[7] J.D. Kirkpatrick, Annu. Rev. Astron. Astrophys. 43 (2005) 195–245.
[8] A. Burrows, W.B. Hubbard, J.I. Lunine, J. Liebert, Rev. Mod. Phys. 73 (2001) 719–765.
[9] S. Lepine, M.M. Shara, R.M. Rich, Astrophys. J. 585 (2003) L69–L72.
[10] S. Lepine, R.M. Rich, M.M. Shara, Astrophys. J. 591 (2003) L49–L52.
[11] A.J. Burgasser, K.L. Cruz, J.D. Kirkpatrick, Astrophys. J. 657 (2007) 494–510.
[12] J.E. Gizis, Astron. J. 113 (1997) 806–822.
[13] D. Petitprez, B. Lemoine, C. Demuynck, L.M. Destombes, B. Macke, J. Chem. Phys. 91 (1989) 4462–4467.
[14] C.I. Frum, H.M. Pickett, J. Mol. Spectrosc. 159 (1993) 329–336.
[15] C.I. Frum, J.J. Oh, E.A. Cohen, H.M. Pickett, Astrophys. J. 408 (1993) L61–L64.
[16] W.L. Barclay Jr., M.A. Anderson, L.M. Ziurys, Astrophys. J. 408 (1993) L65–L67.
[17] A. Shayesteh, K.A. Walker, I. Gordon, D.R.T. Appadoo, P.F. Bernath, J. Mol. Struct. 695 (2004) 23–37.
[18] T.C. Steimle, J. Gengler, J. Chen, Can. J. Chem. 82 (2004) 779–790.
[19] T.C. Steimle, J. Chen, J. Gengler, J. Chem. Phys. 121 (2004) 829–834.
[20] J. Chen, J. Gengler, T.C. Steimle, J.M. Brown, Phys. Rev. A 73 (2006) 012502.
[21] J. Chen, T.C. Steimle, J. Chem. Phys. 128 (2008) 144312.
[22] J.D. Weinstein, R. deCarvalho, T. Guillet, B. Friedrich, J.M. Doyle, Nature 395 (1998) 148–150.
[23] N. Honjou, M. Takagi, M. Makita, K. Ohno, J. Phys. Soc. Jpn. 50 (1981) 2095–2100.
[24] G. Chambaud, B. Lévy, J. Phys. B 22 (1989) 3155–3165.
[25] A. Boutalib, J.P. Daudey, M.E. Mountadi, Chem. Phys. 167 (1992) 111–120.
[26] T. Leininger, G.-H. Jeung, J. Chem. Phys. 103 (1995) 3942–3949.
[27] P.F. Weck, P.C. Stancil, K. Kirby, J. Chem. Phys. 118 (2003) 9997–10005.
[28] F. Holka, M. Urban, Chem. Phys. Lett. 426 (2006) 252–256.
[29] I.S.K. Kerkines, A. Mavridis, J. Phys. Chem. 111 (2007) 371–374.
[30] B. Grundström, Z. Phys. 75 (1932) 302–312.
[31] W.W. Watson, R.L. Weber, Phys. Rev. 48 (1935) 732–734.
[32] W. Whaling, W.H.C. Anderson, J. Brault, H.A. Zarem, J. Res. Natl. Inst. Stand. Technol. 107 (2002) 149–169.
[33] J.M. Brown, E.A. Colbourn, J.K.G. Watson, F.D. Wayne, J. Mol. Spectrosc. 74 (1979) 294–318.
[34] M. Douay, S.A. Rogers, P.F. Bernath, Mol. Phys. 64 (1988) 425–436.
[35] C. Amiot, J.-P. Maillard, J. Chauville, J. Mol. Spectrosc. 87 (1981) 196–218.
[36] G.D. Bell, M. Herman, J.W.C. Jones, E.R. Peck, Phys. Scripta 20 (1979) 609–616.
[37] T. Gustavsson, L. Klynning, B. Lindgren, Phys. Scripta 31 (1985) 269–274.